

The Solar Acoustic Spectrum and Eigenmode Parameters

F. Hill P. B. Stark R. T. Stebbins E. R. Anderson H. M. Antia T. M. Brown
T. L. Duvall, Jr. D. A. Haber J. W. Harvey D. H. Hathaway R. Howe
R. P. Hubbard H. P. Jones J. R. Kennedy S. G. Korzennik A. G. Kosovichev
J. W. Leibacher K. G. Libbrecht J. A. Pinar E. J. Rhodes, Jr. J. Schou
M. J. Thompson S. Tomczyk C. G. Toner R. Toussaint W. E. Williams

December 6, 1996

F. Hill, E. Anderson, J. Harvey, R. Hubbard, J. Kennedy, J. Leibacher, J. Pinar, C. Toner, R. Toussaint, and W. Williams, National Solar Observatory, National Optical Astronomy Observatories, P.O. Box 26732, Tucson AZ 85726-6732, USA. P. Stark, Department of Statistics and Space Sciences Laboratory, University of California, Berkeley, CA 94720-3860, USA. R. Stebbins and D. Haber, JILA, University of Colorado, Boulder, CO 80309-0440, USA. H. Antia, Tata Institute of Fundamental Research, Bombay, India. T. Brown and S. Tomczyk, High Altitude Observatory, National Center for Atmospheric Research, P.O. Box 3000, Boulder, CO 80307-3000, USA. T. Duvall, NASA/GSFC, Stanford University, CSSA, HEPL Annex, Stanford, CA 94305-4085, USA. D. Hathaway, NASA/MSFC, Mail Code ES82, Huntsville, AL 35812, USA. R. Howe and M.J. Thompson, Queen Mary & Westfield College, Mile End Road, London E1 4NS, England. H. Jones, NASA/GSFC Southwest Station, NOAO, P.O. Box 26732, Tucson, AZ 85726-6732, USA. S. Korzennik, Harvard-Smithsonian Center for Astrophysics, 60 Garden St., Cambridge, MA 02138, USA. A. Kosovichev and J. Schou, Stanford University, CSSA, HEPL Annex, Stanford, CA 94305-4085, USA. K.G. Libbrecht, California Institute of Technology, 264-33, Pasadena, CA 91125, USA. E. Rhodes, University of Southern California, Dept of Physics & Astronomy, Los Angeles, CA 90089, USA.

Abstract

The GONG Project estimates the frequencies, amplitudes, and line widths of more than 250,000 acoustic resonances of the Sun from data sets lasting for 36 days. The frequency resolution of a single data set is $0.321 \mu\text{Hz}$. For m -averaged frequencies the median formal error is $0.044 \mu\text{Hz}$, and the associated median fractional error is 1.6×10^{-5} . For a three-year data set, the fractional error is expected to be 3×10^{-6} . GONG m -averaged frequency measurements differ from other helioseismic data sets by 0.03 to $0.08 \mu\text{Hz}$. The differences arise from a combination of systematic errors, random errors, and possible changes in solar structure.

Several million resonant acoustic normal modes (eigenmodes) of the Sun are excited stochastically in the subsurface turbulent layer. The frequencies (ν), amplitudes (A), and characteristic widths (Γ) of such modes, as a function of radial order (n), spherical harmonic degree (l) and azimuthal order (m), comprise the basic data from which helioseismic inferences about the solar interior are drawn. The GONG project currently estimates those eigenspectral parameters for about 250,000 normal modes every 36 days, with the potential to estimate parameters for more than 1,000,000 modes. Here we discuss solar oscillation spectra and random and systematic errors in the estimated mode parameters, and compare GONG mode frequency estimates to those derived from three other experiments.

The amplitudes of solar oscillations are sufficiently small that linear oscillation theory is an excellent approximation. Nonetheless, there are numerous statistical problems in estimating the mode parameters from the surface motions of the Sun as observed through the GONG instruments. These problems include estimating the geometry of the images of the solar disk; estimating the modulation transfer function (MTF) of the instrument and atmosphere; estimating systematic and stochastic components of the observational noise; optimally combining observations obtained at different sites into coherent time series; dealing with missing observations; and estimating parameters of a three-dimensional power spectrum, and their errors and covariances. Because we observe only a portion of one side of the Sun, some power leaks across spatial frequencies and this leakage makes it difficult to separate modes and distinguish splitting caused by solar structure from artifacts of the observation and reduction process. The Sun changes on time scales of 1 month, so common statistical prescriptions, based on frequency resolution and variance, for partitioning the years-long data into shorter time series and combining their spectra do not apply directly; new methods are called for. Similarly, the stochastic nature of the excitation process could be exploited to improve eigenspectral estimates, and statistical properties of the excitation process are interest-

ing themselves. Our knowledge of the solar interior will become more precise as improved statistical techniques, tailored specifically to this problem, are developed and applied to the growing body of GONG data. The current limitation on the accuracy and precision of helioseismic estimates of solar structure from GONG data lies in the details of the data reduction.

Solar Oscillation Spectra

A typical three-dimensional solar acoustic spectrum (Fig. 1) at $l = 85$ contains sets of discrete ridges; each set corresponds to a different value of n . Within each set, further ridges are visible. These arise mainly from the approximate decomposition of the motion of the observable part of the Sun into spherical harmonics: since spherical harmonics are not orthogonal over the observed portion of the Sun (somewhat less than a hemisphere), the spectrum at a target degree l_t contains power from adjacent values of l . This power appears at frequencies appropriate to the degrees of the spatial leaks. If it were possible to observe the entire surface of the Sun, these spatial sidelobes would be substantially reduced, but contributions to the sidelobes from projection effects and the horizontal component of the oscillatory velocity field would remain. GONG spectra have fewer and smaller artifacts than single-site data, which suffer spectral leakage resulting from periodic interruption of the observations between sunset and sunrise.

The standard GONG data products of network spectra and mode parameters are produced every 36 days to sample (but not be synchronized with) the synodic solar rotation period of 27–32 days. For some purposes it is advantageous to combine data over longer time periods either coherently or incoherently. A coherent analysis concatenates several 36-day time series, preserving phase information. This increases the frequency resolution, but does not reduce stochastic noise. As shown in Fig. 2, resolution is improved significantly for modes with long lifetimes (small Γ); these modes typically have low ν . GONG will produce spectra from 1-year time series for $l \leq 30$. Data

can also be combined incoherently by averaging together power spectra from several months. This reduces the stochastic noise, producing a smoother spectrum, but does not increase the frequency resolution. A combination of these approaches allows one to reduce the bias from poor frequency resolution and the variance from stochastic excitation and other sources of noise, but there is a practical upper limit to the length of time series, beyond which we will incur bias from temporal changes in solar properties.

Sources of Error and Uncertainty

There are many sources of uncertainty: external (1), instrumental (2), and data processing (3). To evaluate errors in the GONG eigenfrequency estimates, we used band-passed rms power images to study the differences in velocity noise patterns at different frequencies. At high frequencies, the rms velocity is independent of azimuth and shows a small increase near the center resulting from small residual image motion convolved with the pattern of solar intensity structures (which is strongest near the center of the image), and photon counting noise (which increases towards the limb). At p-mode frequencies, the power has a somewhat larger increase near the center because the velocity of p modes is predominantly normal to the solar surface. At lower frequencies, the rms values are larger near the limb because supergranule flow velocities are predominantly horizontal. A formal propagation of photon and camera read-out noise through the velocity calibration shows that the non-oscillatory solar background contribution is at least two orders of magnitude higher than the camera noise for most values of l and ν .

Differences between estimates derived from stations simultaneously observing the Sun measure uncertainties attributable to instrument and calibration effects, image rotation, estimates of the modulation transfer function, geometric corrections, and image registration. The relative power in the difference of spherical harmonic time series derived from two stations observing the Sun at the

same time is typically low in the p-mode band (Fig. 3). Thus the differences between instruments, and errors in MTF estimates, geometry estimates, image registration, and restored images values, are small. The dominant source of the residual differences is image registration: the location and angular orientation of the image of the Sun on the CCD which is estimated for each image in an early stage of data reduction.

A major source of uncertainty is in estimating mode parameters from the spectra. Mode parameters ν , A , and Γ are estimated from the spectrum by maximizing an approximation to the likelihood function, on the assumption that the spectrum is a superposition of Lorentzian peaks (4). The combination of stochastic variability, spectral leakage resulting from incomplete spatial coverage, and variable signal-to-noise ratio (SNR) as a function of l and ν , can make it difficult to estimate mode parameters accurately (Fig. 4). However, spectra from the network have very small temporal sidelobes, thus fewer peaks to fit, and smaller systematic errors compared with single-site data.

Currently, the GONG project estimates parameters of modes with $\nu \approx 1.5 - 5$ mHz, l between 0 and 150, and all relevant values of m . This represents only about 25% of the modes that contribute to the observed spectra, which include $0 \leq l \leq 250$ and $0 \leq \nu \leq 8.33$ mHz. The restricted region includes all modes that live long enough to be global (producing discrete peaks in the power spectrum), where spatial aliasing is weak, and where the SNR is high. Above $l \approx 180$, modes are local short-lived oscillations with broader line widths, and the frequency spacing between oscillations with adjacent l decreases; as a result, the peaks blend into ridges.

While measurements of $\nu(l, m, n)$ are used to infer the solar angular velocity and asphericity as a function of depth and latitude (5,6), it is also useful to average ν over m (Fig. 5). Averaging reduces the noise in the estimate of ν , and the averaged frequencies can be used to estimate the radial stratification of the density, speed of sound, and the chemical composition in the solar interior

with higher accuracy (6). However, the effect of rotation (which gives rise to the curvature of the ridges in Fig. 1) must be removed before averaging, otherwise the m -averaged mode widths will be overestimated. The effect of rotation is removed by frequency shifting the spectrum for each m (5).

Currently, the reported errors in the mode parameter estimates are formal, and reflect primarily the sensitivity of the parameter-fitting algorithm in the neighborhood of the estimate. Using a 36-day times series of observations, the median formal error in the m -averaged frequencies is about 44 nHz (about 0.14 of one resolution element in ν), and the median fractional error is 1.6×10^{-5} . These errors should decrease as the frequency resolution improves. For 1-year time series, the mean formal error is expected to be about 14 nHz (a fractional error of 5×10^{-6}); over the first three years of the project a mean formal error of 8 nHz (fractional error of 3×10^{-6}) is expected.

While the peak-fitting algorithm assumes that every peak has a specific symmetric shape and background, both are asymmetric in some regions of the spectrum (7). Neglecting these effects probably introduces a small systematic error in the estimated frequencies. The effect of the starting values on the peak-fitting algorithm has been explored by starting the algorithm from randomly generated values about the reference frequencies. The resulting frequency estimates changed on the average by less than 5% of their nominal uncertainties for modes with frequencies in the range 1.8 mHz—3.3 mHz.

Comparison With Other Data Sets

A number of earlier experiments have measured parameters of the modes observed by GONG (8). We examined the differences between m -averaged frequencies obtained by GONG and three other experiments (9), as well as differences between two months of GONG data (Fig. 6). Mode frequencies estimated from Big Bear Solar Observatory (BBSO) data obtained at a time of comparable solar activity differ from GONG estimates by a mean of 29 nHz, with a standard deviation

(SD) of 86 nHz. Mode frequency estimates from LOWL data, obtained about 1 year before GONG, differ from GONG estimates by a mean of 74 nHz with $SD = 81$ nHz. Data from Mt. Wilson and GONG are virtually coeval; their mean difference is 48 nHz, and $SD = 110$ nHz. Although the mean differences are smaller than the standard deviations of the differences, suggesting that the deviations are consistent with zero, Fig. 6 shows that the GONG frequency estimates are systematically lower than those of the other three experiments.

The differences between the GONG results and the others represent a combination of systematic errors, random errors, possible changes in solar structure and dynamics, and variations in solar activity. Evolving solar magnetic activity can produce temporal variations in mode frequencies because the frequencies depend on the level of surface activity (10). These effects also contribute to changes in the GONG frequency estimates from month to month.

The effects of solar changes are substantially eliminated in the Mt. Wilson-GONG comparison since the data were collected simultaneously. Their difference is probably dominated by a combination of unknown systematic errors in both data sets. There is also indication that the difference depends on ν in both the Mt. Wilson-GONG and the LOWL-GONG comparisons. While the actual causes of the frequency differences remain uncertain, GONG's higher duty cycle compared with the other experiments reduces temporal-gap artifacts and improves the SNR. The MTF correction could contribute to the differences; it is applied in the GONG analysis but none of the others. Other details of the data analysis, such as the peak-fitting algorithm and the m -averaging, also play a role.

Comparing spectral estimates from two months of GONG data estimates the reproducibility of m -averaged frequencies obtained by GONG. The mean difference is 3.7 nHz with $SD = 66$ nHz. The SD is about a factor of $\sqrt{2}$ larger than the median of the error estimated by the fitting procedure for one month (44 nHz). Systematic errors should be essentially identical in both data sets, and

the contribution of activity should be small and similar for both months, because solar activity is near minimum.

The identification and estimation of systematic errors is one of the major statistical challenges in helioseismology. Systematic errors in the estimated frequencies result in comparable errors in the inference of solar structure and dynamics. The SOHO-SOI experiment was launched in December 1995 (11) and will provide high- l observations complementary to those obtained by GONG. Comparison of SOI and GONG data will provide estimates of the systematic errors in both data sets.

References and Notes

1. External sources include: other solar velocity fields; attenuation of the oscillations in active regions; terrestrial atmospheric transparency variations (including birds and other opaque objects in the field of view); and seeing and atmospheric scattering.

2. Instrumental sources include: prefilter nonlinearity and drift; image rotator encoder errors; spatial aliasing; spurious modulation; camera nonlinearity and zero level variations; nonlinearity of velocity and intensity during integration; and image cache differences.

3. Data processing sources include: calibration; image geometry determination; remapping residuals from refraction, line-of-sight velocity projection, and pixellation; ephemeris errors; spherical harmonic approximation to true eigenfunctions; merging errors from MTF approximation and velocity scale factors; gap-filling; and peak fitting: leakage, parametric model, algorithm.

4. E. Anderson, T. Duvall, S. Jefferies, *Astrophys. J.* **364**, 699 (1990). For other approaches to estimating mode parameters, see S. Korzennik, thesis, University of California at Los Angeles (1990); J. Schou, thesis, University of Aarhus (1992); K. T. Bachmann, T. L. Duvall, Jr., J. W. Harvey, F. Hill, *Astrophys. J.* **443**, 837 (1995); J. Patr3n, thesis, Universidad de La Laguna (1994).

5. M. J. Thompson *et al.*, *Science*, (1996), and references therein.

6. D. O. Gough *et al.*, *Science*, (1996), and references therein.

7. Observations indicate substantial deviations of the line profile from a symmetrical Lorentzian shape. The line asymmetry is particularly pronounced for low- and high-frequency p modes. The degree of the asymmetry depends on the location of the excitation sources of oscillations relative to the mode resonant cavity (T. L. Duvall, Jr. *et al.*, *Astrophys. J.* **410**, 829 (1993); M. Gabriel, *Astron. Astrophys.* **299**, 245 (1995)).

8. Observational helioseismology has an extensive literature. A very short list of representative papers from other observational efforts in the last decade: Big Bear Solar Observatory: K. G. Libbrecht, M. F. Woodard, J. M. Kaufman, *Astrophys. J. Suppl.* **74**, 1129 (1990); NSO/South Pole: T. L. Duvall, Jr. *et al.*, *Astrophys. J.* **324**, 1158 (1988); Mt. Wilson/USC: E. J. Rhodes, Jr., A. Cacciani, S. G. Korzennik, *Adv. Space Res.* **11**, No. 4, 17 (1991); Birmingham Solar Oscillation Network (BiSON): Y. Elsworth *et al.*, *Astrophys. J.* **434**, 801 (1994); Université de Nice International Research on the Interior of the SUN (IRIS) Network: S. Loudagh *et al.*, *Astron. Astrophys.* **275**, L25 (1993); HAO Fourier Tachometer: K. T. Bachmann, J. Schou, T. Brown, *Astrophys. J.* **412**, 870 (1993) NSO/High-*l* Helioseismometer: K. T. Bachmann *et al.*, K. T. Bachmann, T. L. Duvall, Jr., J. W. Harvey, F. Hill, *Astrophys. J.* **443**, 837 (1995); U. Hawaii Photometric Oscillations Imager: R. S. Ronan, and B. J. LaBonte, *Solar Phys.*, **149**, 1 (1994). Taiwanese Oscillations Network (TON): D.-Y. Chou *et al.*, *Solar Phys.* **160**, 237 (1995). HAO Low-*l* Instrument (LOWL): S. Tomczyk *et al.*, *Solar Phys.* **159**, 1 (1995).

9. Big Bear Solar Observatory: K. G. Libbrecht, M. F. Woodard, J. M. Kaufman, *Astrophys. J. Suppl.* **74**, 1129 (1990); HAO Low-*l* Instrument (LOWL): S. Tomczyk *et al.*, *Solar Phys.* **159**, 1 (1995). Mt. Wilson/USC: E. J. Rhodes, Jr., A. Cacciani, S. G. Korzennik, *Adv. Space Res.* **11**, No. 4, 17 (1991);

10. The frequencies of the p modes are observed to increase as the surface activity level increases. The frequency shift depends on ν and is about $0.4 \mu\text{Hz}$ for $\nu \approx 3 \text{ mHz}$. The shift is thought to result from a combination of magnetic and temperature effects. Observational papers on the subject include: M. F. Woodard and R. W. Noyes, *Nature* **318**, 449 (1985), E. J. Rhodes, Jr. *et al.*, *Astrophys. J.* **326**, 479 (1988), K. G. Libbrecht and M. F. Woodard, *Nature* **345**, 779 (1990), Y. Elsworth, *et al.*, *Nature* **345**, 322 (1990), M. Anguera Gubau, *et al.*, *Astron. Astrophys.* **255**, 363 (1992), and K. T. Bachmann and T. M. Brown, *Astrophys. J. Lett.* **411**, L45 (1993). There is also evidence for a solar cycle variation in Γ (S. M. Jefferies *et al.*, *Astrophys. J.* **377**, 330 (1991)); and in A (Y. Elsworth *et al.*, *Mon. Not. Roy. Astron. Soc.* **265**, 888 (1993)).

11. P. H. Scherrer *et al.*, *Solar Phys.* **162**, 129 (1995).

12. This work utilizes data obtained by the Global Oscillation Network Group (GONG) project, managed by the National Solar Observatory, a Division of the National Optical Astronomy Observatories, which is operated by AURA, Inc. under a cooperative agreement with the National Science Foundation. The data were acquired by instruments operated by the Big Bear Solar Observatory, High Altitude Observatory, Learmonth Solar Observatory, Udaipur Solar Observatory, Instituto de Astrofísica de Canarias, and Cerro Tololo Interamerican Observatory.

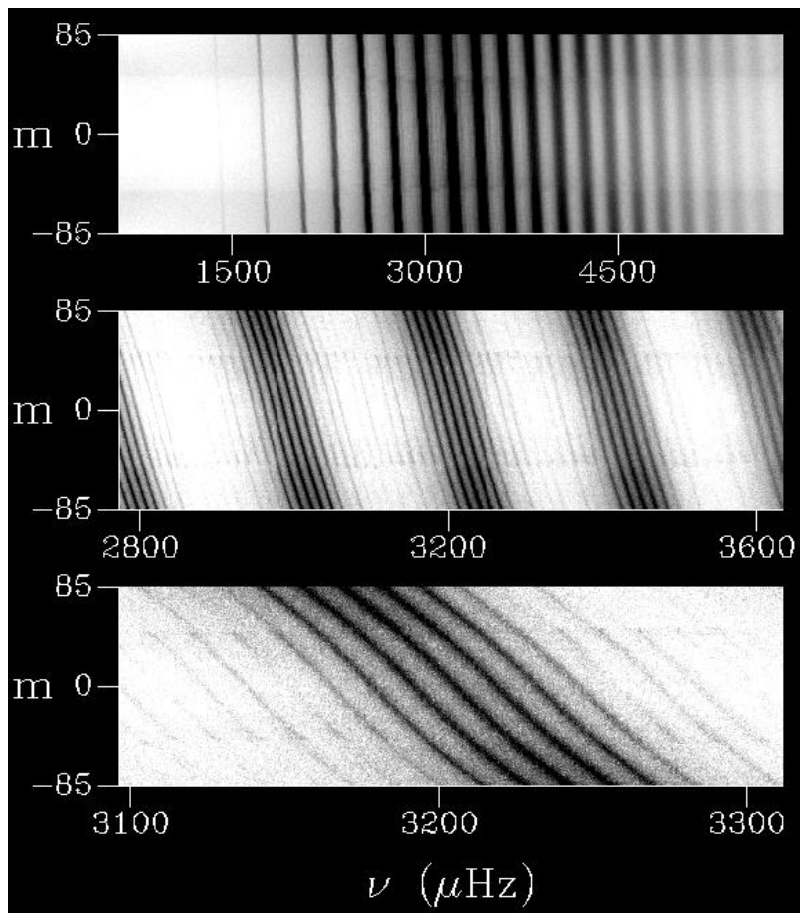


Fig. 1: An example of an $m - \nu$ spectrum for $l = 85$ obtained between 23 Aug. 1995 and 18 Feb. 1996). The spectrum is shown at three magnifications to display the spatial sidelobes that result from observing only a fraction of the solar surface.

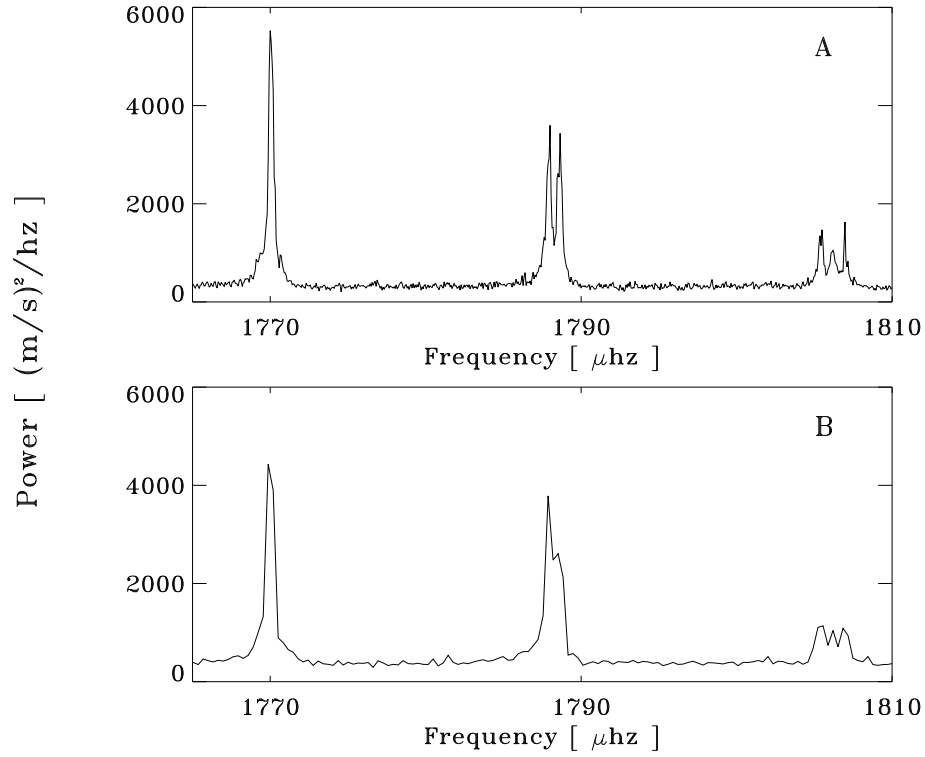


Fig. 2: A demonstration of the increase in frequency resolution of a frequency-shifted m -averaged spectrum resulting from concatenating longer data strings coherently. A: a portion of the oscillation spectrum obtained from a 180-day time series. B: the same portion from a 36-day time series. The fine structure in the peaks arising from leakage with modes at different m is more clearly resolved in the spectrum of the longer time series.

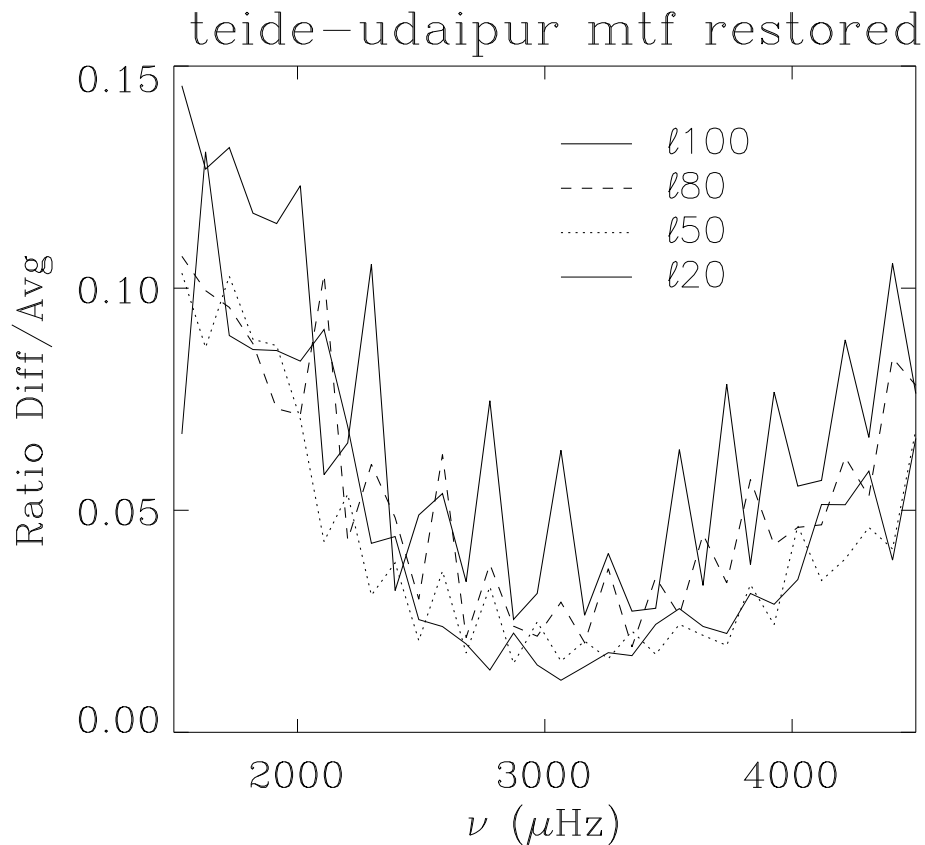


Fig. 3: Power spectrum of the difference between simultaneous observations of the Sun at different sites, normalized by the average power at the two sites. This plot provides a measure of the errors in the power spectra arising from variations between instruments, seeing, pointing, and data processing.

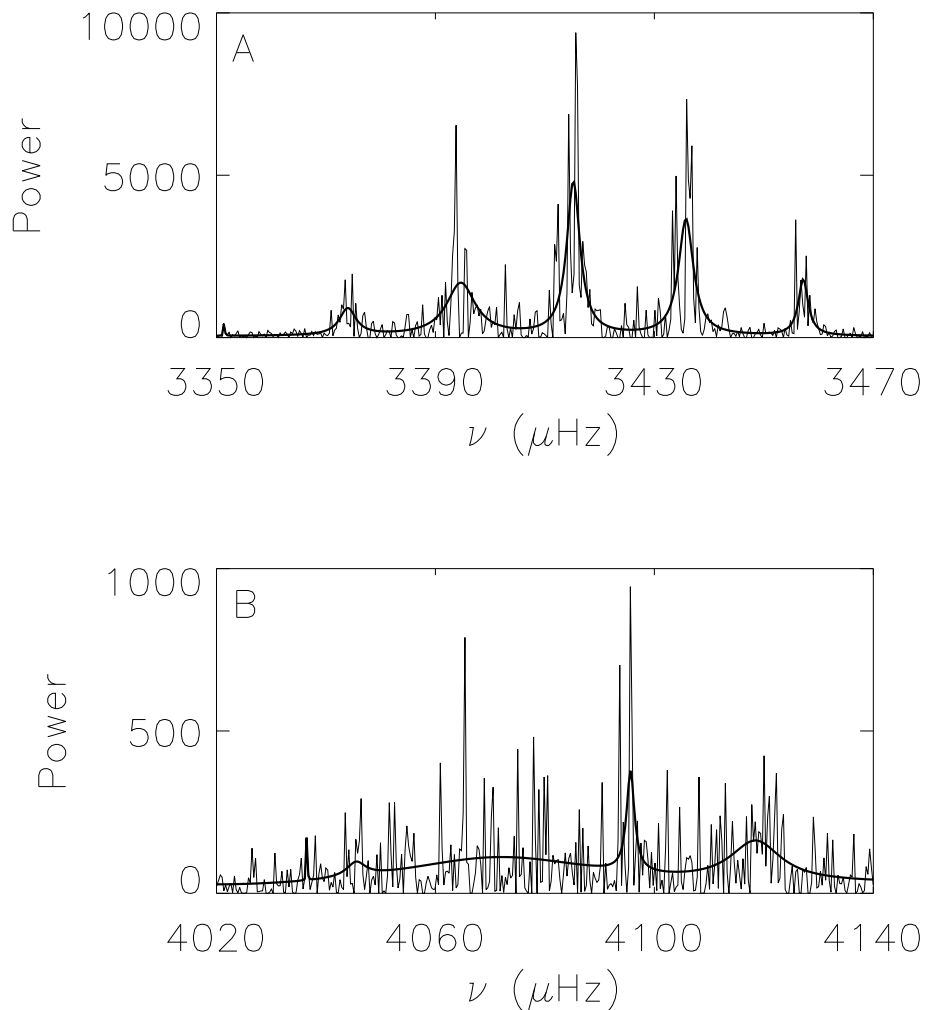


Fig. 4: Two examples of power spectra of spherical harmonic time series and the parametric functions fitted to them to estimate the frequencies, amplitudes, and linewidths of the normal modes they contain. A: a high-quality fit at $l = 50$, $m = -32$, $n = 12$; the uncertainty in the estimated mode parameters is small. B: a poor fit at $l = 50$, $m = 0$, $n = 16$; the estimated parameters were automatically flagged as untrustworthy. Note the different power levels in these spectra.

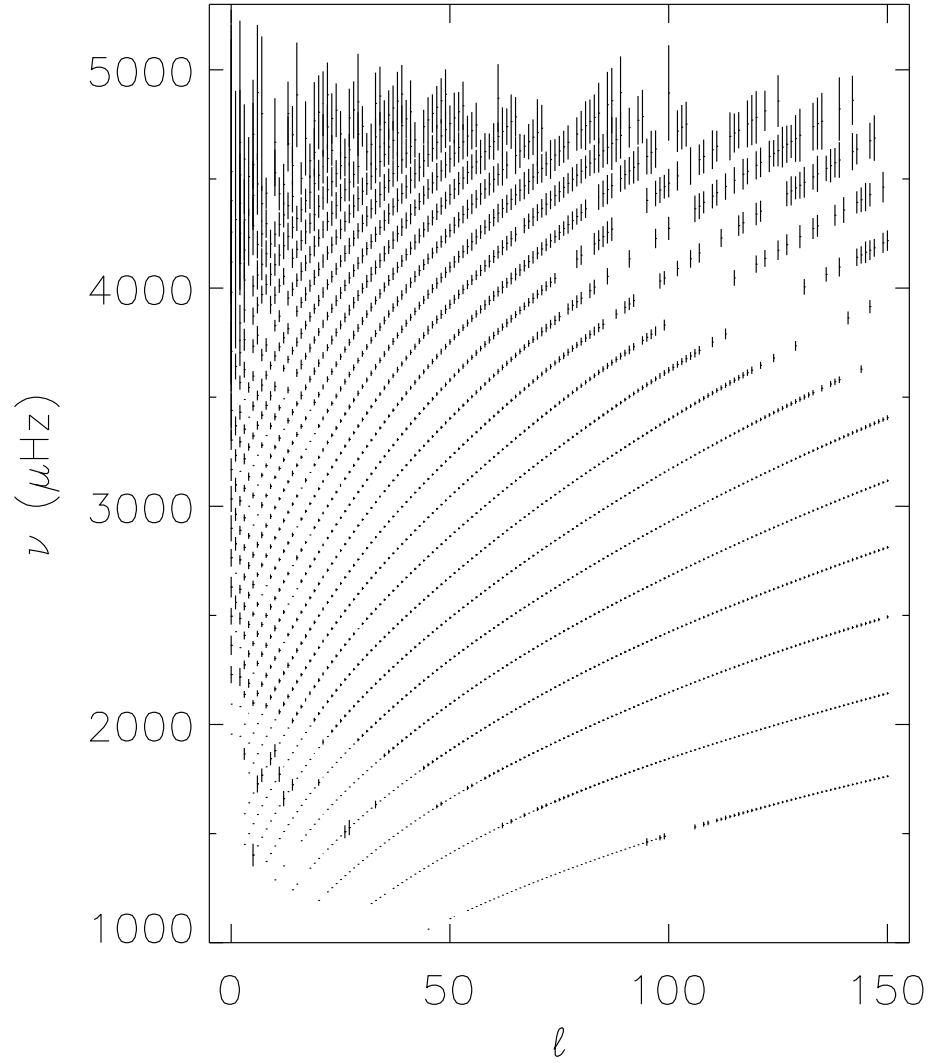


Fig. 5: Central frequencies ν averaged over m measured between 28 Sep. 1995 and 3 Nov. 1995. The errors bars represent the formal errors of the fitted frequencies multiplied by a factor of 200.

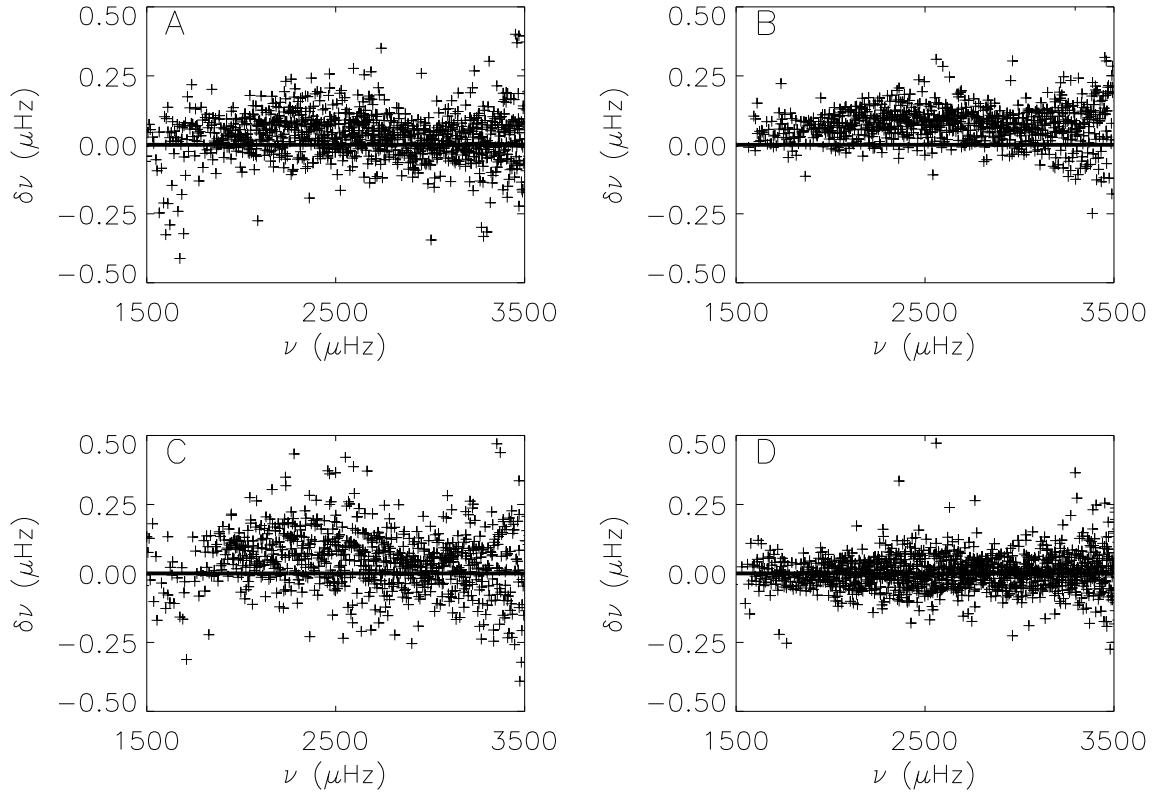


Fig. 6: Comparisons of the GONG m -averaged frequencies obtained between 23 Aug. 1995 and 27 Sep. 1995 with other experiments. A: comparison with estimates from Big Bear Solar Observatory data recorded in 1986. B: comparison with estimates from LOWL data collected between Feb. 26, 1994, and Feb. 25, 1995. C: comparison with estimates from coeval Mt. Wilson data obtained between Aug. 23 and Sep. 27, 1995. D: comparison with estimates from GONG data obtained between Sep. 28 and Nov. 3, 1995.